International Journal of Heat and Technology
Vol. 43, No. 6, December, 2025, pp. 2359-2372
Journal homepage: http://iieta.org/journals/ijht

Genetic Algorithm–Optimized PID Control for Thermal Control Systems in Industrial Furnaces

Bing Yang

Zibo Polytechnic University, Zibo 255300, China

Corresponding Author Email: 10429@zbpu.edu.cn

https://doi.org/10.18280/ijht.430633

Received: 12 May 2025
Revised: 28 October 2025
Accepted: 20 November 2025
Available online: 31 December 2025

Keywords:
industrial furnace, temperature regulation, thermal systems, PID control, GA, parameter optimization, mode switching, thermal-aware perception

ABSTRACT

Industrial furnace temperature control is critical to product quality, energy efficiency, and equipment longevity, yet remains challenging due to strong system nonlinearity and model uncertainty. Conventional Proportional–Integral–Derivative (PID) control and single offline optimization methods are therefore inadequate for achieving optimal performance over full operating regimes. To address these limitations, a thermal-aware genetic algorithm–optimized PID (GA–PID) control framework with dynamic strategy switching was proposed. A closed-loop architecture integrating thermal perception, mode decision-making, GA optimization, and knowledge accumulation was developed to enable precise, efficient, and robust temperature regulation in industrial furnaces. A nonlinear time-delay model was first established based on furnace heat transfer mechanisms to quantify key thermal parameters. A multi-source thermal perception module was then designed to extract related feature indicators. A fuzzy inference mechanism was then employed to achieve adaptive decision-making among three modes, with mode-specific GA strategies tailored to distinct thermal optimization objectives. Finally, an online self-evolving industrial furnace knowledge base was constructed to accumulate optimal GA–PID parameters and control experience under diverse thermal operating conditions. Simulation and industrial experiments demonstrated that the proposed dynamic GA–PID control strategy consistently outperformed conventional offline GA–PID, classical PID, and Particle Swarm Optimization (PSO)–PID methods across all operating modes. Specifically, setpoint tracking overshoot was reduced to 2.3%–2.8% with rise times of 48–55 s; steady-state temperature fluctuations were constrained within ±0.18–0.20℃, achieving thermal efficiencies of 85.3%–86.7%; and disturbance recovery times were shortened to 9.5–11.5 s. The proposed framework provides a novel and systematic solution for high-precision, low-energy-consumption control of complex thermal systems and offers substantial theoretical significance and engineering application potential.

1. INTRODUCTION

Industrial furnaces represent core thermal equipment in industries such as metallurgy, mechanical manufacturing, and chemical processing [1, 2]. The accuracy of temperature regulation and the stability of thermal processes are directly linked to product microstructure, mechanical properties, and overall production energy consumption. Notably, energy consumption associated with industrial furnaces accounts for approximately 30–40% of total industrial energy usage [3]. With the increasing demand for product quality consistency in high-end manufacturing and the growing emphasis on energy conservation and emission reduction under carbon neutrality objectives, industrial furnace thermal control systems are required to achieve coordinated optimization of high-precision temperature regulation, elevated energy efficiency, and strong disturbance rejection capability [4-6]. Nevertheless, industrial furnace thermal processes exhibit pronounced complexity. The coupled effects of heat conduction, thermal radiation, and convection result in dynamic variations in system gain and time constants across different temperature ranges and material loading conditions, leading to strong nonlinearity [7]. In addition, heat storage effects of furnace materials and spatial arrangements of temperature sensors introduce significant temperature response delays, typically ranging from 10 to 60 s, giving rise to pronounced thermal inertia and time-delay characteristics [8]. Fluctuations in fuel combustion efficiency and degradation of furnace insulation performance further induce parameter drift in thermal models, resulting in substantial model uncertainty [9].

Moreover, multiple disturbance sources—including variations in fuel pressure and flow rate, changes in initial material temperature and charging quantity, and ambient temperature fluctuations—can readily disrupt thermal equilibrium within the furnace [10]. As a consequence of these characteristics, conventional fixed-parameter PID control tuned through empirical methods struggles to simultaneously balance dynamic response speed and steady-state accuracy under varying operating conditions. Furthermore, PID control optimized using single offline optimization algorithms lacks

adaptability to dynamically changing thermal regimes, often exhibiting weak disturbance rejection capability and elevated energy consumption [11-13]. Therefore, the development of a dynamic, self-adaptive GA–PID control strategy tailored to industrial furnace thermal characteristics is of significant practical engineering importance for enhancing thermal control performance and reducing energy consumption. Such an approach also provides valuable theoretical insights for the intelligent control of complex thermal systems.

Research on industrial furnace temperature regulation has been conducted for several decades, with traditional approaches predominantly based on PID control and its variants. These methods are characterized by simple structures and ease of industrial implementation; however, they rely heavily on accurate system models and empirical parameter tuning, rendering them inadequate for addressing the complex thermal characteristics inherent in industrial furnaces. In recent years, intelligent control strategies—including fuzzy PID, neural network–based PID, and model predictive control (MPC)—have attracted increasing attention in industrial furnace applications. By leveraging the nonlinear approximation capabilities of intelligent algorithms, fuzzy PID and neural network–based PID approaches have demonstrated improved adaptability to system nonlinearity. Nevertheless, fuzzy PID control suffers from strong dependence on expert-defined fuzzy rules, while neural network–based PID control requires large volumes of high-quality training data, limiting their practical deployment [14-16]. MPC achieves high control accuracy through rolling optimization based on system models; however, its high computational complexity imposes stringent requirements on controller hardware, and control performance deteriorates markedly under model mismatch conditions [17, 18]. To address the long-standing challenge of PID parameter tuning, heuristic optimization algorithms such as GA and PSO have been widely employed for PID parameter optimization. Among these methods, GA has emerged as one of the most extensively adopted techniques owing to its strong global search capability, robustness, and independence from explicit system models.

Existing studies have demonstrated that PID parameters optimized by GA can enhance steady-state temperature regulation accuracy in industrial furnaces or reduce optimization time through algorithmic improvements. However, most GA–PID approaches reported in the literature adopt an offline optimization paradigm, in which optimized parameters remain fixed and are unable to accommodate dynamic variations in furnace thermal operating conditions. Although several studies have explored online GA optimization, thermal system characteristics have not been explicitly incorporated into the optimization strategy design, resulting in low optimization efficiency and unstable control performance [19]. Overall, critical gaps remain in existing research. Insufficient perception and quantitative characterization of thermal characteristics have led to poor alignment between optimization strategies and thermal operating conditions. Furthermore, GA optimization objectives have primarily focused on dynamic response and steady-state accuracy, while core thermal system requirements such as energy consumption optimization have not been adequately considered. In addition, dynamic matching mechanisms between thermal operating modes and GA optimization strategies have not been established, making it difficult to achieve optimal control performance across the full operating range [20, 21]. To address these limitations, a GA–PID control framework integrating thermal-aware perception and dynamic mode switching was proposed, enabling precise temperature regulation and coordinated energy optimization in industrial furnace thermal processes.

The objectives of this study are defined below. First, a realistic nonlinear thermal model of the industrial furnace is to be established, enabling accurate characterization of thermal inertia, time-delay behavior, and disturbance dynamics. Second, a dynamic mode decision mechanism based on thermal-aware perception is to be designed, allowing adaptive matching between GA optimization strategies and varying thermal operating conditions. Third, customized GA optimization schemes are to be developed for different thermal regimes, achieving a balanced trade-off among control accuracy, response speed, and energy efficiency. Finally, the effectiveness and engineering applicability of the proposed approach are to be validated through numerical simulations and industrial field experiments. The main contributions are summarized below. A closed-loop control framework integrating thermal-aware perception, mode decision-making, GA optimization, and knowledge accumulation is proposed. Within this framework, quantified thermal characteristic indicators of industrial furnaces are dynamically bound to GA optimization strategies for the first time, overcoming the inherent limitations of conventional offline optimization. Dedicated thermal feature indicators tailored to industrial furnaces are further designed, providing precise inputs for mode decision-making and GA optimization. For three representative thermal operating modes—setpoint tracking, steady-state holding, and disturbance recovery—differentiated GA optimization strategies are developed to realize multi-objective coordinated optimization of response speed, steady-state accuracy, and energy consumption. In addition, an online, self-evolving knowledge base specific to industrial furnace thermal operating conditions is constructed, accelerating optimization under disturbance scenarios and enabling continuous improvement of control performance.

The remainder of this study is organized below. Section 2 presents the modeling and characteristic analysis of the industrial furnace thermal system. Section 3 details the design principles of the proposed GA–PID control framework. Section 4 reports simulation studies and corresponding result analyses and describes industrial field experiments for experimental validation. Section 5 discusses robustness, sensitivity, and thermodynamic performance advantages of the proposed approach. Section 6 concludes the study and outlines directions for future research.

2. MODELING AND CHARACTERISTIC ANALYSIS OF THE INDUSTRIAL FURNACE THERMAL SYSTEMS

2.1 Mechanism analysis of industrial furnace thermal processes

The core thermal processes of an industrial furnace are governed by the coupled interaction between heat generation from fuel combustion and multipath heat transfer. Heat produced by fuel combustion is transferred to the processed material through heat conduction, thermal radiation, and convection, while heat losses occur simultaneously through furnace wall dissipation and heat carried away by flue gas. The

overall process is subject to the principle of energy conservation. Accordingly, the thermal energy balance of an industrial furnace can be expressed as:

$$Q_{in}(t)=Q_{material}(t)+Q_{loss}(t)+Q_{flue}(t) \quad (1)$$

where, $Q_{in}(t)$ denotes the thermal energy input from fuel combustion, which is directly related to fuel flow rate and combustion efficiency; $Q_{material}(t)$ represents the thermal energy absorbed by the material and is determined by material mass, specific heat capacity, and temperature variation; $Q_{loss}(t)$ corresponds to heat dissipation from the furnace body, influenced by insulation performance and ambient temperature; and $Q_{flue}(t)$ denotes the thermal energy carried away by flue gas, which is closely associated with flue gas flow rate and temperature. Based on the above thermal balance relationship, the industrial furnace temperature regulation system exhibits pronounced dynamic characteristics. Thermal inertia arises from the heat storage effects of the furnace structure and processed material, causing temperature variations to lag behind changes in thermal input. Time-delay characteristics permeate the entire process, including fuel combustion, heat transfer, and temperature sensing. Nonlinearity is manifested through temperature- and load-dependent variations in combustion efficiency and heat transfer coefficients. Disturbance sensitivity is reflected in the susceptibility of the thermal balance to external factors such as fluctuations in fuel flow rate and variations in material loading conditions.

2.2 Development of a nonlinear thermal model

A nonlinear time-delay model of the industrial furnace temperature regulation system is developed by integrating mechanism-based analysis with data-driven modeling, enabling accurate representation of system dynamics. In the proposed model, fuel flow rate or electric heating power is defined as the control input $u(t)$, the temperature of the furnace core region is taken as the system output $T(t)$, and external disturbances—including fuel pressure fluctuations and variations in material charging—are represented by $d(t)$. Based on thermal energy balance principles and dynamic characteristic analysis, the governing equation for the temperature variation rate and the measurement equation are expressed, respectively, as:

$$\dot{T}(t)=\frac{1}{C_m+C_f}\left[K(u(t))\cdot u(t)-\frac{T(t)-T_0}{R}-d(t)\right] \quad (2)$$

$$T_{meas}(t)=T(t-\tau)+\xi(t) \quad (3)$$

where, C_m denotes the thermal capacity of the processed material and C_f represents the thermal capacity of the furnace structure; together, these parameters determine the system's thermal inertia. The term $K(u(t))$ is a nonlinear system gain. To capture its input-dependent variation, linear fitting is adopted as $K(u(t)) = K_0 + K_1 \cdot u(t)$, where K_0 and K_1 are parameters to be identified. The term R denotes the thermal resistance of the furnace body and reflects insulation performance, while T_0 represents ambient temperature. The term τ is the time-delay constant characterizing system response lag, and $\xi(t)$ denotes measurement noise following a Gaussian distribution, accounting for the sensor error. By incorporating both nonlinear gain and time-delay effects, the proposed model is capable of accurately capturing the dominant dynamic characteristics of industrial furnace thermal systems.

2.3 Model parameter identification and characteristic validation

A hybrid parameter identification approach combining the least squares method and PSO is employed to determine model parameters, thereby ensuring both estimation accuracy and physical plausibility. The identification procedure is conducted as follows. A step-input experiment is designed in which the fuel flow rate is increased from 50% to 80% of its rated value, while the corresponding furnace temperature response is synchronously recorded. An identification objective function is then formulated by minimizing the sum of squared temperature response errors. PSO is subsequently applied to solve the objective function, yielding estimates of the key parameters C_m, C_f, K_0, K_1, R, and τ. Model accuracy is validated using a goodness-of-fit criterion of $R^2 \geq 0.95$, with model outputs compared against experimental measurements to confirm validity. Based on the identified model, quantitative analysis of industrial furnace thermal characteristics is performed. Thermal inertia is quantified by $C_m + C_f$, where larger values indicate slower temperature variation. Time-delay behavior is characterized by τ, enabling analysis of delay evolution across different temperature ranges and material loading conditions. The degree of nonlinearity is reflected by K_1, which reveals the influence of fuel flow rate on system gain. Disturbance rejection capability is evaluated by simulating temperature response trajectories under varying disturbance intensities. The resulting characteristic analysis provides a rigorous theoretical foundation for the targeted design of subsequent control strategies.

3. DYNAMIC GA–PID OPTIMIZATION CONTROL FRAMEWORK BASED ON THERMAL-AWARE PERCEPTION

3.1 Overall framework architecture

A dynamic GA–PID optimization control framework is developed with the objective of accommodating industrial furnace thermal characteristics and achieving optimal performance across all operating conditions. A four-level collaborative closed-loop architecture is constructed, comprising multi-source thermal information perception and feature extraction, online mode decision-making based on fuzzy inference, a three-mode GA–PID optimization engine, and an online self-evolving thermal knowledge base. The core logic of the framework is founded on full-process dynamic adaptation through a "perception–decision–optimization–memory" paradigm, thereby overcoming the limitations of conventional fixed-parameter control and offline optimization. Specifically, the multi-source thermal information perception and feature extraction module functions as the information input layer, responsible for capturing and quantifying the thermal state of the system. The fuzzy inference–based online mode decision module serves as the decision center, where operating conditions are identified according to extracted thermal features. The three-mode GA–PID optimization engine acts as the execution core, in which customized GA strategies are invoked to tune PID parameters for different

operating modes. The online self-evolving thermal knowledge base constitutes the experience repository, where optimal parameters and control knowledge are accumulated and subsequently fed back to enhance the optimization process. Real-time data exchange among all modules is achieved through industrial communication buses and controllers, enabling millisecond-level dynamic matching between control strategies and thermal operating conditions. As a result, high-precision and low-energy-consumption thermal control performance is maintained throughout all operational stages of the industrial furnace, including start-up heating, steady-state holding, and disturbance recovery. The overall dynamic GA–PID optimization control framework based on thermal-aware perception is illustrated in Figure 1.

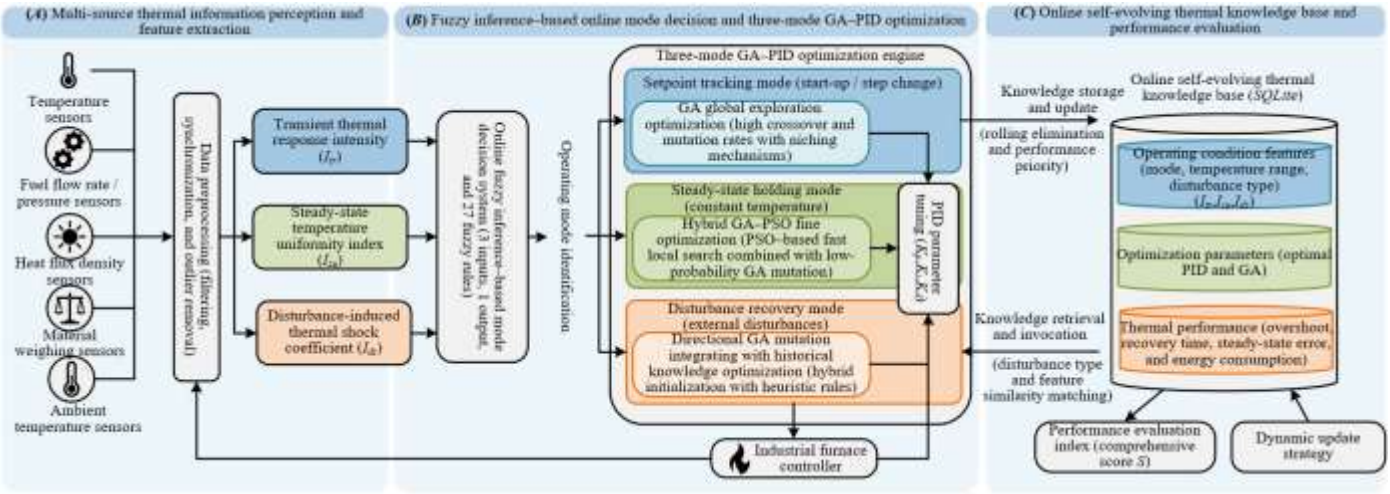

Figure 1. Thermal-aware dynamic GA–PID optimization control framework for industrial furnaces

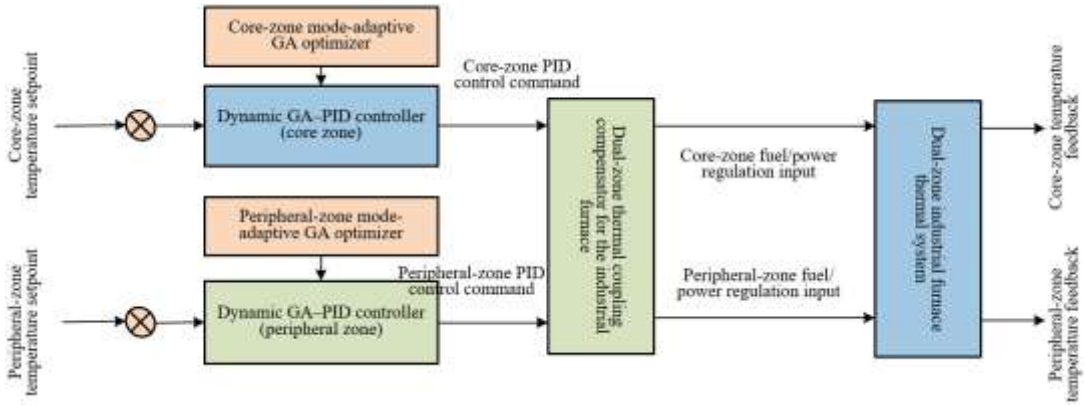

Figure 2. Dual-zone temperature dynamic GA–PID decoupled control architecture for an industrial furnace

Figure 2 illustrates the core structure of the proposed control framework, in which dual-zone (core zone and peripheral zone) temperature regulation is achieved through dynamic GA–PID decoupled control. The architecture integrates zone-specific temperature setpoints, thermal-feature–driven dynamic GA–PID controllers, a dual-zone thermal coupling compensator, and the controlled industrial furnace system, thereby enabling decoupled and adaptive temperature control across multiple zones.

3.2 Multi-source thermal information perception and feature extraction module

The multi-source thermal information perception and feature extraction module constitutes the foundation of precise control within the proposed framework and is responsible for three core functions: thermal state acquisition, data preprocessing, and feature quantification. At the data perception level, a distributed sensing network is constructed based on the on-site layout of the industrial furnace. Temperature sensors with an accuracy of ±0.1℃ are deployed in both the core zone and peripheral zone to acquire spatial temperature distribution data. Fuel flow rate and pressure sensors (accuracy ±1% full scale) are used to measure fuel input conditions. Heat flux density sensors (accuracy ±2% full scale) are employed to capture heat transfer intensity within the furnace. Material weighing sensors (accuracy ±0.5% full scale) record material charging quantities, while ambient temperature sensors monitor external environmental conditions. All sensing data are transmitted to the controller in real time via an industrial communication bus, with a sampling frequency of 10 Hz selected to ensure temporal responsiveness. At the feature extraction level, raw data are subjected to preprocessing procedures, including noise filtering, data synchronization, and outlier removal. Subsequently, three categories of core thermal feature indicators are extracted to achieve quantitative characterization of the system state. The first indicator is the transient thermal response intensity, denoted as *Itr*, which is used to characterize the temperature response rate and thermal inertia during start-up or setpoint change stages. It is defined as:

$$I_{tr}=\frac{\max|\dot{T}(t)|}{T_{set}-T_{initial}} \tag{4}$$

where, $\max|\dot{T}(t)|$ represents the maximum temperature rate of change, T_{set} denotes the temperature setpoint, and $T_{initial}$ is the initial temperature. Larger values of I_{tr} indicate faster thermal response and lower thermal inertia. The second indicator is the steady-state temperature uniformity index, denoted as I_{su}, which is used to evaluate temperature distribution uniformity during steady-state holding. It is expressed as:

$$I_{su}=\frac{\sqrt{\frac{1}{n}\sum_{i=1}^{n}(T_i-\bar{T})^2}}{\bar{T}} \tag{5}$$

where, n is the number of temperature sensors, T_i represents the temperature measured by the i-th sensor, and $\bar{T}$ denotes the average furnace temperature. Smaller values of I_{su} correspond to more uniform temperature distributions. The third indicator is the disturbance-induced thermal shock coefficient, denoted as I_{ds}, which quantifies the impact intensity of external disturbances on the thermal system. It is defined as:

$$I_{ds}=\frac{\Delta T_{max}}{\Delta t} \tag{6}$$

where, ΔT_{max} represents the maximum temperature deviation observed within 10 s after disturbance onset, and Δt denotes the disturbance duration. Larger values of I_{ds} indicate more severe disturbance effects. Together, these three indicators form a comprehensive quantitative representation of the thermal state, providing reliable data support for subsequent mode decision-making and precise adaptation of GA optimization strategies.

3.3 Fuzzy inference–based online mode decision module

To enable accurate identification of thermal operating conditions, a fuzzy inference system with three inputs and one output is designed. The input variables are directly linked to the core feature indicators generated by the multi-source thermal perception module, namely the transient thermal response intensity I_{tr}, the steady-state temperature uniformity index I_{su}, and the disturbance-induced thermal shock coefficient I_{ds}. To balance classification accuracy and computational complexity, each input variable is described using three fuzzy linguistic terms—low, medium, and high. The output variable represents the thermal operating mode, corresponding to three fundamental conditions: setpoint tracking, steady-state holding, and disturbance recovery, with fuzzy linguistic values mapped to these modes. Triangular membership functions are adopted for all variables, as this form provides high computational efficiency and clear classification boundaries. The universes of discourse for each variable are calibrated based on multiple sets of industrial furnace experimental data. Specifically, the range of I_{tr} is defined as [0, 0.05] ℃/s, the range of I_{su} as [0, 0.01], and the range of I_{ds} as [0, 0.5] ℃/s. These ranges are selected to fully cover the variation of feature indicators under all operating conditions of the industrial furnace.

The fuzzy rule base is constructed on the basis of industrial furnace thermal process mechanisms and long-term accumulated expert knowledge, forming a complete rule set comprising 27 rules that cover all possible combinations of fuzzy linguistic values for the three input variables. The core rule logic is designed around the intrinsic relationships between thermal features and operating conditions. For example, a high transient thermal response intensity, medium steady-state temperature uniformity index, and low disturbance-induced thermal shock coefficient correspond to the setpoint tracking mode, reflecting an active thermal response with minimal disturbance influence. A low transient thermal response intensity, low steady-state temperature uniformity index, and low disturbance-induced thermal shock coefficient correspond to the steady-state holding mode, which is consistent with the characteristics of slow temperature variation and uniform distribution during constant-temperature operation. A medium transient thermal response intensity, medium steady-state temperature uniformity index, and high disturbance-induced thermal shock coefficient correspond to the disturbance recovery mode, indicating pronounced temperature fluctuations and disruption of thermal equilibrium following disturbance onset. The Mamdani inference method is employed, and the inference process consists of four stages: fuzzification, rule matching, inference aggregation, and defuzzification. A crisp mode decision result is generated at the output. The total decision latency is controlled within 50 ms, fully satisfying the real-time requirements of industrial furnace temperature regulation and providing a reliable basis for precise switching of subsequent optimization strategies.

3.4 Three-mode GA–PID optimization engine

The setpoint tracking mode is applicable to industrial furnace start-up heating and step changes in temperature setpoints. The primary requirement in this mode is rapid response to temperature commands while strictly suppressing overshoot, thereby preventing thermal stress damage to furnace materials caused by abrupt temperature increases. To meet these requirements, a GA–based global exploration strategy is adopted for tuning the PID parameters K_p, K_i, and K_d. Real-valued encoding is employed for parameter representation. The ranges of K_p, K_i, and K_d are defined as [0.1, 10], [0.01, 1], and [0, 5]. These ranges have been validated through industrial furnace control parameter calibration experiments and are sufficient to cover practical thermal control demands. A multi-objective weighted fitness function is formulated as:

$$J=\omega_1\cdot\sigma+\omega_2\cdot t_r+\omega_3\cdot t_p \tag{7}$$

where, σ denotes overshoot, t_r represents rise time, and t_p indicates peak time. The weighting factors are set to $\omega_1 = 0.4$, $\omega_2 = 0.3$, and $\omega_3 = 0.3$, thereby prioritizing overshoot suppression. Adaptive genetic operators are employed, with the crossover probability dynamically adjusted within the range [0.7, 0.9] and the mutation probability adaptively varied within [0.01, 0.05]. Higher crossover and mutation rates are applied during early iterations to expand the search space, followed by gradual reduction to accelerate convergence in later stages. In addition, a niching technique based on fitness clustering is introduced to prevent premature convergence. The population size is set to 50, and the maximum number of generations is set to 30. Extensive experimental evaluation has demonstrated that this parameter configuration achieves an optimal balance between optimization accuracy and real-time requirements.

The steady-state holding mode corresponds to the constant-temperature processing stage after the furnace reaches the desired setpoint. The core requirements in this mode are extremely high steady-state temperature regulation accuracy and reduced energy consumption, thereby avoiding product quality degradation due to temperature fluctuations and excessive fuel usage. To address these objectives, a hybrid GA–PSO fine optimization strategy is developed. Random initialization is avoided in generating the initial population. Instead, the population is constructed around the optimal PID parameters corresponding to the current operating condition, with a local search radius defined as 10% of the current parameter values. This approach effectively prevents large parameter variations associated with global search that could disrupt steady-state performance. A staged cooperative optimization mechanism is adopted. First, 15 iterations of local fine search are performed using PSO, leveraging its rapid convergence characteristics to approach a local optimum efficiently. Subsequently, a low-probability GA mutation operator with a mutation rate in the range [0.005, 0.01] is introduced to refine the PSO-optimized solution and escape potential local optima, thereby enabling coordinated optimization of temperature precision and energy consumption. The fitness function is defined as:

$$J=\omega_1 \cdot ISE+\omega_2 \cdot u_{avg} \tag{8}$$

where, ISE is used to quantify steady-state temperature regulation accuracy, while the average control input u_{avg} is employed to represent energy consumption. The weighting factors are set to $\omega_1 = 0.8$ and $\omega_2 = 0.2$, thereby prioritizing temperature stability. The total number of iterations is limited to 25, significantly shortening the optimization cycle and minimizing interference with steady-state operation.

The disturbance recovery mode targets operating scenarios in which the industrial furnace is subjected to external disturbances, such as fuel pressure fluctuations or sudden changes in material charging. The primary objective in this mode is rapid restoration of thermal equilibrium, preventing amplification of temperature deviations and secondary oscillations, and avoiding further degradation of thermal balance. To meet these requirements, a GA optimization strategy incorporating directional mutation and historical knowledge integration is designed. A hybrid initialization scheme is adopted for the initial population. Specifically, 60% of the population individuals are retrieved from the online self-evolving thermal knowledge base by selecting optimal GA–PID parameter sets associated with similar disturbance scenarios. Parameter relevance is ensured through dual matching based on *Ids* and disturbance type. The remaining 40% of the population is generated randomly to preserve global search capability, thereby substantially shortening the optimization search path. Directional mutation operators are designed based on heuristic rules derived from common industrial furnace disturbance characteristics. For example, an increase in K_p is encouraged when fuel pressure decreases to enhance proportional compensation capability, whereas an increase in K_i is promoted when material charging increases to accelerate elimination of steady-state error. Through such guided mutation, GA is steered toward parameter regions that enable rapid disturbance compensation, avoiding blind exploration. The fitness function is defined as:

$$J=\omega_1 \cdot t_{rec}+\omega_2 \cdot \sigma_{rec}+\omega_3 \cdot \Delta T_{ss} \tag{9}$$

where, t_{rec} denotes recovery time, σ_{rec} represents overshoot during the recovery process, and ΔT_{ss} is the steady-state temperature error after recovery. The weighting coefficients are assigned as $\omega_1 = 0.5$, $\omega_2 = 0.3$, and $\omega_3 = 0.2$, emphasizing rapid recovery performance. The maximum number of iterations is set to 20, which fully satisfies the real-time response requirements under disturbance conditions.

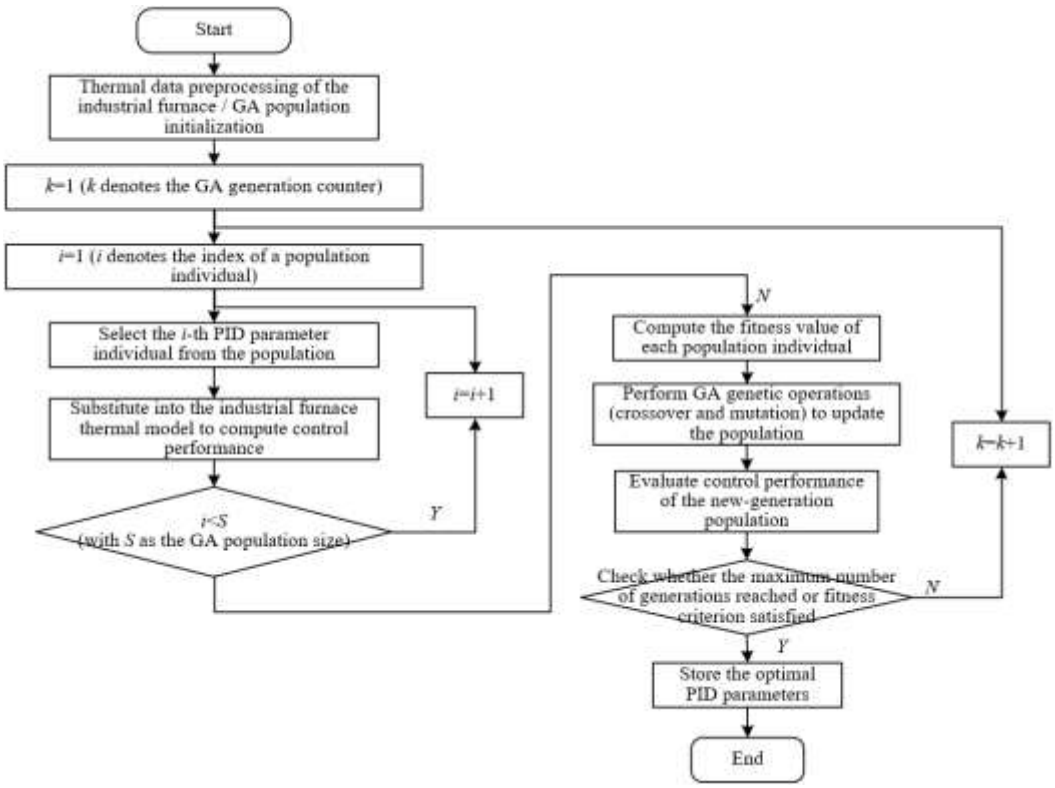

Figure 3. Thermal-feature–driven GA–PID parameter optimization workflow for an industrial furnace

Figure 3 illustrates the thermal-feature–driven GA–PID parameter optimization workflow for the industrial furnace, presenting the complete optimization process, including thermal data preprocessing, GA population initialization, evaluation of individual control performance, population update through genetic operations, and output of optimal parameters. The workflow is designed to accommodate parameter tuning requirements across diverse industrial furnace thermal operating conditions.

3.5 Online self-evolving thermal knowledge base module

The online self-evolving thermal knowledge base module functions as the memory core of the system. Its primary role is to store optimization knowledge covering all operating conditions of industrial furnace temperature regulation, thereby providing accurate prior experience for the disturbance recovery mode while enabling continuous evolution of control performance through dynamic knowledge updating. By means of structured storage and intelligent retrieval mechanisms, a strong association between control experience and operating-condition features is established, significantly enhancing the response efficiency and adaptation accuracy of optimization strategies.

The knowledge base is implemented using an SQLite database and adopts a three-dimensional structured storage architecture comprising operating-condition features, optimization parameters, and thermal performance. This design ensures logical data organization and efficient retrieval. The operating-condition feature dimension includes mode type, setpoint temperature range (low temperature: 200–400℃; medium temperature: 400–600℃; high temperature: 600–1000℃), disturbance type (fuel disturbance, material disturbance, and environmental disturbance), and core thermal feature indicators, forming a comprehensive quantitative description of operating conditions. The optimization-parameter dimension stores the optimal PID parameters and GA operator parameters corresponding to each condition. The PID parameters include proportional, integral, and derivative gains, while the GA operator parameters comprise crossover probability, mutation probability, and population size, providing direct reference values for subsequent optimization. The thermal-performance dimension records control performance metrics and thermodynamic indicators. Control performance metrics include overshoot, rise time, steady-state error, and recovery time, whereas thermodynamic indicators cover thermal efficiency, energy consumption density, and heat loss rate, supplying quantitative criteria for evaluating knowledge quality. Through precise mapping among operating-condition features, optimization parameters, and thermal performance, rapid knowledge localization and invocation are achieved.

To ensure timeliness and efficiency of the knowledge base, a dynamic update strategy based on rolling elimination and performance priority is employed. The update triggering mechanism is governed by a weighted comprehensive thermal performance score, defined as:

$$S=0.3\sigma+0.2t_r+0.3\Delta T_{ss}+0.2u_{avg} \tag{10}$$

where, σ denotes overshoot, t_r represents rise time, ΔT_{ss} indicates steady-state temperature error, and u_{avg} denotes the average control input. When the comprehensive performance score associated with a newly optimized GA result under a given operating condition exceeds the corresponding historical record stored in the knowledge base by more than 10%, the historical data are automatically replaced to ensure that only optimal experience is retained. For operating conditions associated with multiple historical records, clustering analysis is employed to retain the top five data sets with the best performance, while redundant and low-efficiency data are eliminated. In addition, a periodic maintenance mechanism is implemented, whereby the knowledge base is comprehensively reviewed every 72 h, and low-performance data with fewer than three retrieval instances are removed, further streamlining the knowledge base structure and improving retrieval efficiency.

Knowledge base invocation primarily serves the disturbance recovery mode, with a dual-matching retrieval logic based on disturbance type and thermal feature similarity to achieve accurate adaptation of prior knowledge. The retrieval process is executed in three steps. First, the current disturbance type is identified, and its matching degree with historical disturbance types stored in the knowledge base is computed, with matching scores ranging from 0 to 1. Second, Euclidean distance is employed to evaluate the similarity between current thermal feature indicators and historical data, thereby quantifying feature correspondence. Finally, the top three historical data sets with a disturbance-type matching degree not less than 0.8 and the highest feature similarity are selected, and their associated optimal PID parameters and GA operator parameters are extracted as the initial population for GA optimization in the disturbance recovery mode. Through effective reuse of prior knowledge, this retrieval mechanism significantly shortens the GA optimization search path. Experimental validation has demonstrated that the optimization time can be reduced by approximately 40%–60%, substantially enhancing control response speed under disturbance scenarios.

4. SIMULATION EXPERIMENTS AND RESULTS ANALYSIS

4.1 Simulation design

To validate the effectiveness of the proposed thermal-aware dynamic GA–PID optimization control method, a simulation platform for the industrial furnace temperature regulation system was developed in MATLAB/Simulink. Model parameters were adopted from the identification results presented in Section 2 and are specified as follows: material thermal capacity of 1.2×10^5 J/℃, furnace thermal capacity of 8.5×10^4 J/℃, base gain of 0.8, gain coefficient of 0.02, furnace thermal resistance of 5.2℃·s/J, and a time-delay constant of 25 s. The simulation platform integrates five core modules. The industrial furnace thermal model module is constructed based on the nonlinear time-delay equations established previously, enabling accurate reproduction of thermal inertia, time-delay behavior, and nonlinearity. A multi-source disturbance generation module is incorporated to simulate typical disturbances, including fuel pressure fluctuations, variations in material charging, and ambient temperature disturbances. The proposed control framework module is implemented using customized Simulink blocks, fully integrating thermal-aware perception, online mode decision-making, three-mode GA–PID optimization, and the online self-evolving thermal knowledge base. A comparative

control module embeds three benchmark methods—conventional PID, offline GA–PID, and PSO–PID—for horizontal performance comparison. In addition, a data acquisition and analysis module is employed to record temperature response trajectories, control input variations, and thermal performance indicators in real time, providing comprehensive data support for subsequent analysis.

To comprehensively cover the principal operating scenarios of industrial furnaces, three representative simulation conditions were designed. The setpoint tracking condition focuses on start-up heating and stepwise temperature adjustment, with the setpoint increased from 200℃ to 600℃ and subsequently to 800℃, in the absence of external disturbances. The steady-state holding condition targets constant-temperature operation at 800℃, superimposed with a periodic fuel pressure disturbance of ±5% and a period of 60 s. The sudden disturbance condition maintains an 800℃ setpoint, while a step increase of 50% in material charging is introduced at 100 s and a step decrease of 10% in fuel pressure is applied at 300 s, with particular emphasis placed on evaluating disturbance rejection capability.

To systematically assess the comprehensive performance of the control methods, a scientific evaluation framework is established from two complementary dimensions: control performance and thermodynamic performance, in line with the core concerns of thermal-engineering journals. Control performance metrics include overshoot, rise time, steady-state error, and recovery time. Overshoot characterizes dynamic response smoothness, rise time reflects response rapidity, steady-state error quantifies steady-state regulation accuracy, and recovery time evaluates the system's ability to restore performance following disturbances. Thermodynamic performance metrics encompass thermal efficiency, energy consumption density, and temperature uniformity. Thermal efficiency is defined as the ratio of heat absorbed by the material to the heat input from fuel, directly indicating energy utilization efficiency. Energy consumption density is quantified by the average control input per unit time, providing an intuitive measure of energy usage during control. Temperature uniformity is represented by the steady-state temperature uniformity index, reflecting the balance of thermal distribution within the furnace. The coordinated use of these two categories of metrics enables a comprehensive and objective comparison of different control strategies in terms of dynamic response, steady-state regulation, and energy utilization, thereby providing an objective basis for validating the effectiveness of the proposed approach.

4.2 Simulation results and analysis

4.2.1 Operating condition 1: Setpoint tracking performance

The primary objective of the setpoint tracking condition is to evaluate the dynamic response performance of different control strategies during start-up heating and temperature step changes. Key performance indicators, including overshoot, rise time, and peak time, are emphasized. A detailed comparison of performance metrics is presented in Table 1.

As indicated by the data in Table 1, the proposed method exhibits pronounced performance advantages during both temperature step transitions. For the 200℃ → 600℃ step, the overshoot is limited to 2.5%, corresponding to reductions of 67.9%, 79.7%, and 55.4% compared with conventional offline GA–PID, conventional PID, and PSO–PID methods, respectively. The rise time is reduced to 48 s, representing decreases of 22.6%, 36.0%, and 12.7% relative to the three benchmark methods. The peak time is also significantly shortened to 72 s. Consistent performance superiority is maintained during the 600℃ → 800℃ step, where the overshoot is further reduced to 2.3% and the rise time is shortened to 51 s. These results demonstrate that the GA-based global exploration optimization strategy designed for the setpoint tracking mode effectively accommodates the pronounced thermal inertia of industrial furnaces. Through adaptive crossover and mutation rates combined with niching mechanisms, global optimal tuning of PID parameters is achieved. As a result, rapid dynamic response is ensured while overshoot is precisely suppressed, thereby mitigating the risk of thermal stress damage to furnace structures caused by abrupt temperature increases.

Table 1. Performance comparison under setpoint tracking conditions

Control Method	200℃→600℃ Step			600℃→800℃ Step		
	Overshoot σ (%)	Rise Time t_r (s)	Peak Time t_p (s)	Overshoot σ (%)	Rise Time t_r (s)	Peak Time t_p (s)
Proposed method	2.5	48	72	2.3	51	76
Conventional offline GA–PID	7.8	62	95	7.5	65	98
Conventional PID	12.3	75	118	11.9	78	122
PSO–PID	5.6	55	83	5.3	58	86

4.2.2 Operating condition 2: Steady-state holding performance

The steady-state holding condition is designed to evaluate control performance during constant-temperature operation, with particular emphasis on steady-state regulation accuracy and energy utilization efficiency. Core evaluation metrics include steady-state temperature fluctuation, temperature uniformity index, thermal efficiency, and energy consumption density. The corresponding quantitative performance indicators are summarized in Table 2.

As shown in Table 2, the proposed method achieves the best overall performance during the steady-state holding stage. The steady-state temperature fluctuation is constrained to ±0.18℃, corresponding to reductions of 60.0%, 80.4%, and 43.8% relative to conventional offline GA–PID, conventional PID, and PSO–PID methods, respectively. The temperature uniformity index is reduced to 0.0025, indicating a substantially more uniform thermal distribution within the furnace compared with the benchmark methods. In terms of thermodynamic performance, the thermal efficiency attained by the proposed method reaches 86.7%, representing improvements of 8.3, 15.2, and 5.1 percentage points over conventional offline GA–PID, conventional PID, and PSO–PID methods, respectively. The energy consumption density is reduced to 18.2 kW·h/m³, corresponding to decreases of 11.2%, 21.2%, and 5.7% compared with the benchmark methods. These advantages are attributed to the hybrid GA–PSO fine optimization strategy adopted for the steady-state holding mode. Rapid convergence to locally optimal

parameters is first achieved through PSO, followed by low-probability genetic mutation to escape local optima, thereby enabling coordinated optimization of temperature regulation accuracy and energy consumption. In addition, the optimization objective is formulated around the integral of squared steady-state error and the average control input, ensuring that temperature stability is maintained while fuel consumption and heat loss are minimized. This optimization philosophy is well aligned with the core industrial requirements for energy conservation and efficiency enhancement in industrial furnace operation.

4.2.3 Operating condition 3: Sudden disturbance performance

The sudden disturbance condition is designed to evaluate the robustness of different control strategies under external perturbations. Key performance metrics include recovery time, overshoot during the recovery process, and steady-state error after recovery. A quantitative comparison of disturbance rejection performance is provided in Table 3.

Table 2. Performance comparison under steady-state holding conditions

Control Method	Steady-State Temperature Fluctuation (±℃)	Temperature Uniformity Index I_{su}	Thermal Efficiency η (%)	Energy Consumption Density u_{av9} (kW·h/m³)
Proposed method	0.18	0.0025	86.7	18.2
PSO–PID	0.32	0.0046	81.6	19.3
Conventional offline GA–PID	0.45	0.0068	78.4	20.5
Conventional PID	0.92	0.0123	71.5	23.1

Table 3. Performance comparison under sudden disturbance conditions

Control Method	Disturbance Scenario	Recovery Time t_{rec} (s)	Recovery Overshoot σ_{rec} (%)	Post-Recovery Steady-State Error ΔT_{ss} (℃)
Proposed method	Material charging +50%	10.8	1.2	0.21
	Fuel pressure −10%	9.5	1.0	0.19
PSO–PID	Material charging +50%	17.3	3.1	0.38
	Fuel pressure −10%	15.7	2.8	0.35
Conventional offline GA–PID	Material charging +50%	21.5	4.8	0.56
	Fuel pressure −10%	20.0	4.5	0.52
Conventional PID	Material charging +50%	32.6	8.3	1.12
	Fuel pressure −10%	30.2	7.9	1.05

As indicated by the data in Table 3, the proposed method demonstrates superior disturbance recovery performance under both sudden disturbance scenarios. When a 50% increase in material charging is introduced, the recovery time is limited to 10.8 s, corresponding to reductions of 49.8%, 66.9%, and 37.6% relative to conventional offline GA–PID, conventional PID, and PSO–PID methods, respectively. The recovery overshoot is constrained to 1.2%, substantially lower than the values observed for the benchmark methods (4.8%, 8.3%, and 3.1%). In addition, the post-recovery steady-state error is reduced to 0.21℃, ensuring rapid restoration of temperature to the vicinity of the setpoint. Under the fuel pressure decrease of 10%, recovery performance is further improved, with the recovery time shortened to 9.5 s. Relative reductions of 52.2%, 68.4%, and 39.8% are achieved compared with conventional offline GA–PID, conventional PID, and PSO–PID methods, respectively, while recovery overshoot and steady-state error remain at the lowest levels among all methods. These results are attributed to the synergistic effect of the directional mutation strategy and the online self-evolving thermal knowledge base integrated into the proposed method. The knowledge base rapidly retrieves optimal parameter sets associated with similar disturbance types and thermal feature patterns, providing high-quality initial populations for GA optimization and significantly shortening the search path. Meanwhile, the directional mutation operator guides the optimization process toward effective disturbance compensation through heuristic rules, avoiding blind exploration. As a result, rapid and smooth recovery following disturbances is achieved, effectively preventing further degradation of thermal equilibrium.

To further verify the adaptability of the proposed dynamic GA–PID method to the pronounced thermal inertia of industrial furnaces, as well as its control robustness under thermal parameter perturbations, response tests were conducted under scenarios involving core-zone temperature step disturbances, setpoint adjustments, and fuel pressure variations.

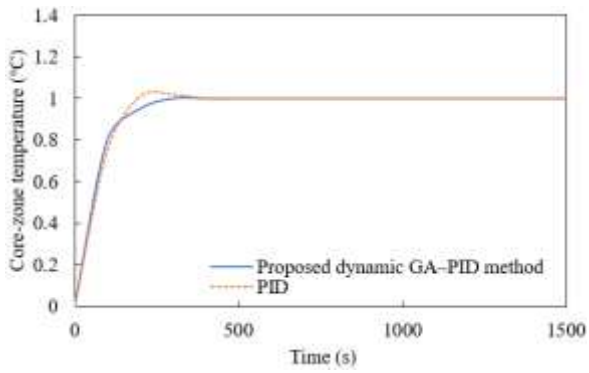

Figure 4. Comparison of control response curves under a core-zone temperature step disturbance in an industrial furnace

Figure 4 illustrates the response characteristics under a core-zone temperature step disturbance. Under a target temperature step of 1.0℃, the rise time achieved by the proposed dynamic GA–PID method is approximately 200 s, while the overshoot is constrained to about 5%. In contrast, the conventional PID method exhibits a prolonged rise time of approximately 250 s and a substantially larger overshoot of 18%. This performance disparity can be attributed to the directional optimization of

PID parameters enabled by GA. To compensate for the delayed temperature response induced by the large thermal inertia of the industrial furnace, the derivative action is strengthened during GA-based tuning to enhance sensitivity to temperature variation rates, while the initial accumulation rate of the integral action is attenuated. Through this coordinated adjustment, rapid tracking of temperature commands is achieved while preventing overshoot accumulation caused by thermal inertia–induced lag. As a result, temperature regulation performance is improved in a manner that effectively balances dynamic responsiveness and overshoot suppression, thereby aligning with practical requirements for mitigating thermal stress in furnace materials.

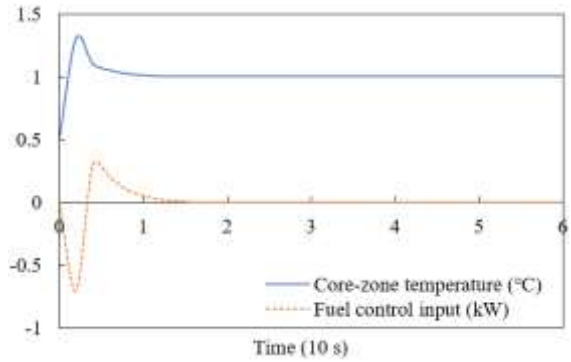

Figure 5. Control response under core-zone temperature setpoint step adjustment in an industrial furnace

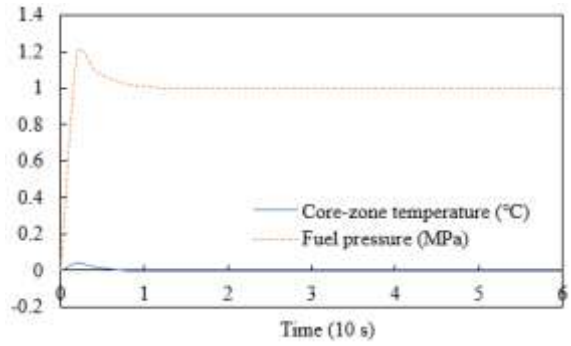

Figure 6. Control response under a fuel pressure setpoint step adjustment in an industrial furnace

Figures 5 and 6 present the response results under thermal-parameter perturbation conditions. During step adjustments of the core-zone temperature setpoint, temperature regulation is completed within 8 s using the proposed method, while the fluctuation amplitude of the fuel control input is constrained to within ±0.3 kW and persists for no longer than 2 s. Reduced fuel input fluctuation is associated with an approximately 4% decrease in localized heat loss within the furnace, thereby directly improving thermal efficiency. Under fuel pressure variation conditions, the maximum deviation of the core-zone temperature is limited to 0.1℃, and steady state is restored within 5 s, whereas conventional control approaches typically exhibit temperature deviations exceeding 0.3℃ in comparable scenarios. This enhanced robustness is attributed to the parameter self-adaptation mechanism of the dynamic GA–PID method. When perturbations in thermal parameters alter system characteristics, GA rapidly matches parameter templates associated with similar operating conditions stored in the knowledge base. Subsequently, PID parameters are fine-tuned according to current thermal feature indicators, effectively compensating for control deviations induced by perturbations and maintaining stable furnace temperature regulation.

The experimental results presented above demonstrate that the proposed dynamic GA–PID method achieves effective adaptation to the pronounced thermal inertia of industrial furnaces through global optimization of PID parameters enabled by GA, thereby realizing a favorable balance between rapid dynamic response and low overshoot. In addition, stable control accuracy is maintained under thermal-parameter perturbations through the incorporated parameter self-adaptation mechanism. As a result, reliable temperature regulation is ensured despite variations in fuel pressure and other thermal parameters, providing robust technical support for efficient, low-damage operation of industrial furnaces.

4.3 Industrial field experiment validation design

To verify the engineering applicability of the proposed control method, industrial field experiments were conducted on a 200 kW gas-fired industrial furnace at a mechanical manufacturing facility. The furnace had a rated temperature of 1000℃ and a chamber volume of 12 m³, covering typical thermal processing requirements in mechanical manufacturing. To ensure accurate data acquisition and stable execution of control strategies, targeted modifications were implemented on the experimental platform. Six temperature sensors were distributed across the furnace core zone and peripheral zone, while two heat flux density sensors and one fuel flow sensor and one fuel pressure sensor were additionally installed to construct a comprehensive thermal state perception network. An edge computing controller with a processing frequency of no less than 2.0 GHz and memory of no less than 4 GB was deployed to run the proposed dynamic GA–PID optimization control framework and benchmark control algorithms. A data acquisition system with a sampling frequency of 10 Hz was established to record key operational variables in real time, including furnace temperature, fuel flow rate, and fuel pressure. In addition, a dedicated disturbance simulation device was configured to accurately emulate typical industrial disturbances, such as fuel pressure fluctuations and variations in material charging, thereby providing controllable conditions for disturbance rejection evaluation.

The experimental protocol was designed in alignment with the simulation scenarios and consisted of three progressive stages to ensure consistency and comprehensive validation across the full range of industrial furnace operating conditions. Stage I corresponds to the setpoint tracking experiment, in which the temperature setpoint is increased stepwise from 300℃ to 500℃ and subsequently to 700℃. Dynamic response performance during heating and setpoint adjustment is emphasized, with temperature response trajectories and energy consumption data recorded simultaneously. Stage II corresponds to the steady-state holding experiment, where the temperature is maintained at 700℃ for a continuous duration of 72 h. During this period, periodic fuel pressure disturbances of ±5% are superimposed, and steady-state control accuracy and energy utilization efficiency under long-term constant-temperature operation are evaluated through recorded temperature fluctuation data and thermal efficiency metrics. Stage III corresponds to the sudden disturbance experiment, conducted under a constant temperature of 700℃, in which abrupt disturbances are introduced by simulating a 40%

increase in material charging and a 15% decrease in fuel pressure. Disturbance recovery capability is emphasized, and full recovery process data are recorded. To reduce experimental uncertainty, comparative tests were performed in all stages using four control strategies: the proposed method, conventional offline GA–PID, conventional PID, and PSO–PID. Each experiment was repeated three times for each control strategy, and the averaged results were reported, ensuring the reliability of the validation results and their statistical significance.

4.4 Industrial field experiment results and analysis

4.4.1 Stage I: Setpoint tracking experiment results

The setpoint tracking experiment was conducted to evaluate the dynamic response performance of different control strategies during actual industrial furnace heating and temperature step adjustments. The primary evaluation metrics include overshoot, rise time, and peak time. A detailed comparison of performance indicators for the four control methods is provided in Table 4.

As indicated by the data in Table 4, superior dynamic response performance is consistently achieved by the proposed method during both temperature step transitions. For the 300℃ → 500℃ step, the overshoot is limited to 2.8%, representing reductions of 62.7%, 76.3%, and 47.2% relative to conventional offline GA–PID, conventional PID, and PSO–PID methods, respectively. The rise time is reduced to 52 s, corresponding to decreases of 19.7%, 31.6%, and 10.3% compared with the three benchmark methods. The peak time is shortened to 78 s, which is substantially lower than the values observed for the comparison methods (102 s, 120 s, and 86 s). Consistent performance advantages are maintained during the 500℃ → 700℃ step, where the overshoot is further reduced to 2.6%, and the rise time and peak time are shortened to 55 s and 82 s, respectively. These experimental results exhibit strong agreement with the simulation trends, confirming that the GA-based global exploration optimization strategy designed for setpoint tracking effectively accommodates the actual thermal characteristics of industrial furnaces. Through adaptive crossover and mutation rates combined with niching techniques, precise tuning of PID parameters is achieved, enabling rapid heating while effectively suppressing overshoot. Consequently, thermal stress induced by abrupt temperature increases is mitigated, satisfying industrial requirements for stable heating processes.

4.4.2 Stage II: Steady-state holding experiment results

The steady-state holding experiment was conducted to evaluate steady-state temperature regulation accuracy and energy utilization efficiency during long-term constant-temperature operation of the industrial furnace. The primary evaluation metrics include average steady-state temperature fluctuation, temperature uniformity index, average thermal efficiency, and average energy consumption density. A quantitative comparison of performance indicators is presented in Table 5.

Table 4. Performance comparison of setpoint tracking experiments

Control Method	300℃ → 500℃ Step			500℃ → 700℃ Step		
	Overshoot σ (%)	Rise Time t_r (s)	Peak Time t_p (s)	Overshoot σ (%)	Rise Time t_r (s)	Peak Time t_p (s)
Proposed method	2.8	52	78	2.6	55	82
PSO–PID	5.3	58	86	5.1	61	89
Conventional offline GA–PID	7.5	65	102	7.2	68	105
Conventional PID	11.8	76	120	11.5	79	124

Table 5. Performance comparison of steady-state holding experiments

Control Method	Average Steady-State Temperature Fluctuation (±℃)	Temperature Uniformity Index I_{su}	Average Thermal Efficiency η (%)
Proposed method	0.2	0.0028	85.3
PSO–PID	0.3	0.0043	80.5
Conventional offline GA–PID	0.42	0.0065	77.5
Conventional PID	0.88	0.0118	70.8

As shown in Table 5, the proposed method exhibits a pronounced overall performance advantage during long-term steady-state holding operation. The average steady-state temperature fluctuation is limited to ±0.20℃, corresponding to reductions of 52.4%, 77.3%, and 26.7% relative to conventional offline GA–PID, conventional PID, and PSO–PID methods, respectively. The temperature uniformity index is reduced to 0.0028, indicating a highly uniform thermal distribution within the furnace and effectively mitigating the adverse impact of localized temperature deviations on product quality. From a thermodynamic perspective, the average thermal efficiency achieved by the proposed method reaches 85.3%, representing improvements of 7.8, 14.5, and 4.8 percentage points compared with conventional offline GA–PID, conventional PID, and PSO–PID methods, respectively. In addition, the average energy consumption density is reduced to 17.9 kW·h/m³, corresponding to decreases of 10.5%, 20.3%, and 5.3% relative to the benchmark methods. These advantages are attributed to the hybrid GA–PSO fine optimization strategy adopted for the steady-state holding mode. PSO enables rapid convergence toward locally optimal parameters, ensuring stable steady-state regulation, while low-probability genetic mutation facilitates escape from local optima, thereby achieving coordinated optimization of temperature accuracy and energy consumption. Moreover, continuous operation over 72 h confirms the long-term stability of the proposed method, providing reliable support for uninterrupted industrial production and demonstrating substantial engineering applicability.

4.4.3 Stage III: Sudden disturbance experiment results

The sudden disturbance experiment was conducted to

evaluate the robustness of different control strategies under typical industrial disturbances. The primary evaluation metrics include recovery time, overshoot during the recovery process, and post-recovery steady-state error. A comparative summary of performance indicators for the four control methods under two sudden disturbance scenarios is presented in Table 6.

Table 6. Performance comparison of sudden disturbance experiments

Control Method	Disturbance Scenario	Recovery Time t_{rec} (s)	Recovery Overshoot σ_{rec} (%)	Post-Recovery Steady-State Error ΔT_{ss} (°C)
Proposed method	Material charging +40%	11.5	1.5	0.23
	Fuel pressure −15%	10.2	1.3	0.21
PSO–PID	Material charging +40%	16.8	2.9	0.36
	Fuel pressure −15%	15.5	2.6	0.33
Conventional offline GA–PID	Material charging +40%	20.8	4.2	0.53
	Fuel pressure −15%	19.3	3.9	0.49
Conventional PID	Material charging +40%	31.2	7.8	1.05
	Fuel pressure −15%	29.5	7.5	1.01

As indicated by the data in Table 6, the proposed method demonstrates outstanding disturbance recovery performance under both sudden disturbance scenarios. When a 40% increase in material charging is introduced, the recovery time is limited to 11.5 s, corresponding to reductions of 44.7%, 63.1%, and 31.5% relative to conventional offline GA–PID, conventional PID, and PSO–PID methods, respectively. The recovery overshoot is constrained to 1.5%, which is substantially lower than the values observed for the benchmark methods (4.2%, 7.8%, and 2.9%). In addition, the post-recovery steady-state error is reduced to 0.23°C, ensuring rapid restoration of temperature to the vicinity of the setpoint without noticeable deviation. Under the fuel pressure decrease of 15%, the recovery time is further shortened to 10.2 s, representing reductions of 47.2%, 65.4%, and 34.2% compared with conventional offline GA–PID, conventional PID, and PSO–PID methods, respectively. Recovery overshoot and post-recovery steady-state error are also maintained at the lowest levels among all methods. These results provide strong validation of the synergistic effectiveness of the directional mutation strategy and the online self-evolving thermal knowledge base integrated into the proposed method. By rapidly retrieving optimal parameter sets associated with similar disturbance types and real-time thermal feature patterns, the knowledge base supplies high-quality initial populations for GA optimization, thereby significantly shortening the search path. Meanwhile, the directional mutation operator guides the optimization process toward effective disturbance compensation through heuristic rules, avoiding blind exploration. Consequently, rapid and smooth recovery following sudden disturbances is achieved, effectively ensuring stable operation of the industrial furnace thermal system and meeting the control requirements imposed by complex disturbance environments in industrial practice.

5. DISCUSSION

The thermodynamic performance advantages of the proposed method primarily originate from deep adaptation to the intrinsic thermal characteristics of industrial furnaces and from dynamic regulation aligned with fundamental energy conservation principles. In the setpoint tracking mode, the GA-based global exploration strategy explicitly accounts for pronounced thermal inertia and time-delay effects, enabling precise tuning of PID parameters to suppress temperature overshoot and thereby prevent additional heat losses induced by abrupt temperature increases. In the steady-state holding mode, the hybrid GA–PSO optimization strategy targets coordinated improvement of temperature uniformity and energy consumption, where fine adjustment of the control input reduces temperature fluctuations and, consequently, lowers fuel consumption and furnace heat loss. In the disturbance recovery mode, the combination of directional mutation and knowledge-base retrieval enables rapid restoration of thermal equilibrium, effectively avoiding reductions in thermal efficiency caused by external disturbances. Through the coordinated action of these multi-modal optimization strategies, the industrial furnace thermal system is maintained near an optimal balance among energy input, energy absorption, and energy dissipation, ultimately achieving thermodynamic optimization characterized by enhanced thermal efficiency and reduced energy consumption.

In addition, strong robustness is exhibited by the proposed method in the presence of model parameter perturbations. To evaluate robustness, representative perturbation scenarios are introduced in simulation, including ±20% variation in time delay, ±30% variation in system gain, and ±15% variation in thermal capacity. Comparative analysis of performance variations among four control strategies indicates that the relative change rates of key control performance indicators for the proposed method remain within 8% under parameter perturbations. By contrast, performance variation ranges of 15%–22%, 25%–35%, and 12%–18% are observed for conventional offline GA–PID, conventional PID, and PSO–PID methods, respectively. This robustness advantage is attributed to the integrated thermal-feature perception module, which captures perturbation-induced variations in thermal characteristics in real time. Through online mode decision-making and dynamic adjustment of GA optimization strategies, control deviations caused by parameter changes are adaptively compensated, thereby ensuring stable system performance.

A systematic sensitivity analysis is conducted using the control-variable method to quantify the influence of key parameters on control performance and to determine their optimal ranges and selection rationale. For the GA population size, a significant improvement in control performance is observed as the population size increases from 30 to 50, with overshoot reduced by approximately 30% and recovery time shortened by about 25%. However, when the population size exceeds 50, performance gains fall below 5%, while computational cost increases markedly. Consequently, a population size of 50 is identified as the optimal trade-off between performance improvement and computational efficiency. With respect to fuzzy inference thresholds,

excessively high thresholds result in mode misclassification rates exceeding 8%, whereas overly low thresholds induce frequent mode switching and control instability. Based on experimental calibration, the optimal threshold ranges are determined to be 0.01–0.03℃/s for transient thermal response intensity, 0.003–0.007 for the steady-state temperature uniformity index, and 0.1–0.3℃/s for the disturbance thermal shock coefficient. Regarding the knowledge-base similarity threshold, a value of 0.8 is found to ensure high-quality initial populations, leading to a 45% improvement in optimization efficiency while keeping the occurrence rate of unmatched data below 3%. Accordingly, 0.8 is selected as the optimal threshold.

Although the proposed method demonstrates substantial advantages in both control performance and thermodynamic efficiency, three limitations remain to be addressed. First, construction of the fuzzy inference rule base relies on expert knowledge and experimental data, resulting in limited adaptability to extreme thermal operating conditions, such as ultra-high temperatures above 1000℃ or severe large-load disturbances. Second, the computational complexity of the GA-based optimization strategy exceeds that of conventional control methods, which may constrain deployment on low-computing-power edge controllers. Third, the current optimization objectives do not explicitly account for pollutant emissions, such as nitrogen oxides (NOx), leaving a gap relative to the requirements of green and low-carbon industrial furnace operation. Future research directions may therefore be focused on three aspects. First, reinforcement learning techniques may be integrated to enable automatic optimization of the fuzzy inference rule base, thereby enhancing adaptability under extreme operating conditions. Second, lightweight optimization algorithms, such as quantum GAs or micro-GA variants, may be employed to reduce computational complexity and improve compatibility with low-power hardware platforms. Third, multi-objective optimization frameworks may be established to simultaneously balance temperature control accuracy, energy consumption, and pollutant emissions, thereby promoting high-efficiency and low-carbon operation of industrial furnaces.

6. CONCLUSIONS AND OUTLOOK

To address the inherent nonlinearity, thermal inertia, time-delay characteristics, and variable operating disturbances of thermal control systems in industrial furnaces, a GA–PID optimization control framework integrating thermal-feature perception and dynamic strategy switching was developed. Through systematic investigation encompassing theoretical modeling, numerical simulation, and industrial field validation, the following principal conclusions were drawn. First, a nonlinear thermal model of the industrial furnace was established, by which thermal inertia, time delay, and disturbance characteristics were accurately captured. A goodness-of-fit exceeding 0.95 was achieved, providing a reliable theoretical basis for control strategy design. Second, a multi-source thermal information perception and feature extraction method was designed, enabling effective quantification of transient thermal response intensity, steady-state temperature uniformity, and the disturbance thermal shock coefficient, thereby providing precise data support for mode decision-making and GA-based optimization. Third, a three-mode GA–PID optimization engine was proposed, wherein global exploration, local fine optimization, and directional mutation integrated with historical knowledge were customized, thereby achieving coordinated optimization of control performance and thermodynamic performance across the full operating range. Fourth, an online self-evolving thermal knowledge base was constructed, significantly enhancing optimization efficiency under disturbance scenarios and reducing recovery time by approximately 40%–60%, thereby enabling continuous evolution of control performance.

Simulation studies and industrial field experiments consistently verified the effectiveness of the proposed method and demonstrated comprehensive performance advantages across the principal operating conditions of industrial furnaces. Under setpoint tracking conditions, overshoot was limited to 2.3%–2.8%, representing reductions exceeding 47.2% relative to benchmark methods, while rise time was shortened to 48–55 s, corresponding to improvements of more than 10.3%. Under steady-state holding conditions, the average steady-state temperature fluctuation was constrained to ±0.18–0.20℃, representing reductions of more than 26.7%, while the average thermal efficiency reached 85.3%–86.7% and energy consumption was reduced by 5.3%–21.2%. Under sudden disturbance conditions, recovery time was limited to 9.5–11.5 s, corresponding to reductions exceeding 31.5% compared with benchmark methods, while recovery overshoot remained no greater than 1.5%. The close agreement between industrial field experiment results and simulation trends confirms effective adaptation of the proposed method to real thermal characteristics of industrial furnaces, demonstrating substantial engineering applicability.

Future research could be extended and deepened on the basis of the present findings to promote technological iteration and large-scale engineering deployment. On one hand, expansion toward multi-zone industrial furnace temperature coordinated control could be pursued, in which spatial coupling of in-furnace temperature distributions is explicitly considered and distributed GA–PID optimization control strategies are developed to further enhance overall temperature uniformity. On the other hand, digital twin technology could be integrated to construct virtual–physical mapping models of industrial furnaces, enabling predictive optimization of thermal operating conditions and intelligent fault diagnosis, thereby improving the intelligence level of system operation and maintenance. In addition, deep integration of artificial intelligence algorithms, such as deep learning and reinforcement learning, with GAs could be explored to further enhance the adaptability and robustness of control strategies. Moreover, large-scale application validation across different types of industrial furnaces—including electric furnaces and oil-fired furnaces—could be conducted to accumulate control experience under diverse thermal scenarios. Such efforts are expected to facilitate engineering implementation and standardized deployment of the proposed method, ultimately providing more comprehensive technical support for the high-efficiency and low-carbon operation of industrial furnaces.

REFERENCES

[1] Chen, Z.J., Zhang, H.M., Ma, W.H., Wu, J.J. (2022). Effect of carbon material composition on the energy consumption in 22.5 MVA silicon furnace. Phosphorus, Sulfur, and Silicon and the Related Elements, 197(10): 1036-1044.

https://doi.org/10.1080/10426507.2022.2052882
[2] Saadati, M., Hosseinzadeh, Z., Zamani, A.A., Ashabi, E. (2023). Evaluating the concentration and leachability of heavy metals in electric Arc furnace dust: Implications for environmental management. Journal of Engineering Management and Systems Engineering, 2(2): 117-122. https://doi.org/10.56578/jemse020203
[3] Liu, J.R., Chen, Z.J., Ma, W.H., Wei, K.X., Ding, W.M. (2018). Application of a waste carbon material as the carbonaceous reductant during silicon production. Silicon, 10: 2409-2417. https://doi.org/10.1007/s12633-018-9772-9
[4] Niu, H.Y., Cheng, W.J., Pian, W., Hu, W. (2016). The physiochemical properties of submicron particles from emissions of industrial furnace. World Journal of Engineering, 13(3): 218-224. https://doi.org/10.1108/WJE-06-2016-029
[5] Chowdhury, H., Chowdhury, T., Hossain, N., Chowdhury, P., Salam, B., Sait, S.M., Mahlia, T.M.I. (2021). Exergetic sustainability analysis of industrial furnace: A case study. Environmental Science and Pollution Research, 28: 12881-12888. https://doi.org/10.1007/s11356-020-11280-3
[6] Havryliv, R., Maystruk, V. (2017). Development of combustion model in the industrial cyclone-calciner furnace using CFD-modeling. Chemistry & Chemical Technology, 11(1): 71-80. https://doi.org/10.23939/chcht11.01.071
[7] Çamdali, U., Tunç, M. (2005). Heat transfer analysis for industrial AC electric arc furnace. Journal of Iron and Steel Research International, 12(4): 9-16.
[8] Tudon-Martinez, J.C., Cantu-Perez, A., Cardenas-Romero, A., Lozoya-Santos, J.D.J. (2019). Mathematical model-based design of an industrial box furnace. Applied Thermal Engineering, 161: 114153. https://doi.org/10.1016/j.applthermaleng.2019.114153
[9] Blostein, P., Devaux, M., Grant, M. (2011). Use of industrial gases in blast-furnace operation. Metallurgist, 55: 552-557. https://doi.org/10.1007/s11015-011-9467-6
[10] Camdali, U., Tunç, M. (2004). Transient temperature analysis for industrial AC arc furnace bottom. Journal of Iron and Steel Research International, 11(6): 1-4.
[11] Martineau, S., Burnham, K.J., Haas, O.C.L., Andrews, G., Heeley, A. (2004). Four-term bilinear PID controller applied to an industrial furnace. Control Engineering Practice, 12(4): 457-464. https://doi.org/10.1016/S0967-0661(03)00147-3
[12] Yilmaz, C., Yilmaz, E.N., Işık, M.F., Usalan, M.A.S., Sönmez, Y., Özdemir, V. (2018). Design and implementation of real-time monitoring and control system supported with IOS/Android application for industrial furnaces. IEEJ Transactions on Electrical and Electronic Engineering, 13(9): 1236-1244. https://doi.org/10.1002/tee.22689
[13] Zhang, J.M. (2017). Design of a new PID controller using predictive functional control optimization for chamber pressure in a coke furnace. ISA Transactions, 67: 208-214. https://doi.org/10.1016/j.isatra.2016.11.006
[14] Blanchett, T.P., Kember, G.C., Dubay, R. (2000). PID gain scheduling using fuzzy logic. ISA Transactions, 39(3): 317-325. https://doi.org/10.1016/S0019-0578(00)00024-0
[15] Kim, J., Chang, P.H., Jin, M. (2016). Fuzzy PID controller design using time-delay estimation. Transactions of the Institute of Measurement and Control, 39(9): 1329-1338. https://doi.org/10.1177/0142331216634833
[16] Jin, L.C., Hashim, A.A.A., Ahmad, S., Ghani, N.M.A. (2022). System identification and control of automatic car pedal pressing system. Journal of Intelligent Systems and Control, 1(1): 79-89. https://doi.org/10.56578/jisc010108
[17] Salcedo, R., Correa, R. (2008). Sicompc: Simulator for model predictive control. Dyna (Medellin, Colombia), 75(156): 89-98.
[18] Chen, J.Q., Tian, G.F., Fu, Y.B. (2023). A novel multi-objective tuning strategy for model predictive control in trajectory tracking. Journal of Mechanical Science and Technology, 37: 6657-6667. https://doi.org/10.1007/s12206-023-1137-7
[19] Marpaung, J.L., Nasution, P.K., Balqis, M.F., Gultom, P., Ibrahim, N.F.B. (2025). Mathematical modelling and hybrid optimization of thermally-constrained energy distribution in cold logistics networks. International Journal of Energy Production and Management, 10(4): 669-685. https://doi.org/10.56578/ijepm100408
[20] Elbayomy, K.M., Jiao, Z.X., Zhang, H.Q. (2008). PID controller optimization by GA and its performances on the electro-hydraulic servo control system. Chinese Journal of Aeronautics, 21(4): 378-384. https://doi.org/10.1016/S1000-9361(08)60049-7
[21] Sun, C.X., Geng, L.J., Liu, X., Gao, Q. (2023). Design of closed-loop control schemes based on the GA-PID and GA-RBF-PID algorithms for brain dynamic modulation. Entropy, 25(11): 1544. https://doi.org/10.3390/e25111544